

# Purification of Waste Carbon for Battery Applications via Ascorbic Acid Leaching

Maria Joriza Cañete Bondoc<sup>1</sup>, Joel Jorolan<sup>1</sup>, Jonah Gamutan<sup>1</sup>, Jacob Martin<sup>2</sup>, Hyung-Sub Eom<sup>3</sup>, Go-Gi Lee<sup>3</sup>, and Richard Diaz Alorro<sup>1,\*</sup>

<sup>1</sup>Western Australian School of Mines: Minerals, Energy and Chemical Engineering, Curtin University, Australia

<sup>2</sup>Department of Physics and Astronomy, Curtin University, Australia

<sup>3</sup>Industrial Materials Research Group Rare Metals Cell, Research Institute of Industrial Science and Technology (RIST), South Korea

**Abstract.** Graphite is increasingly recognized as a critical material with its essential role in clean energy technologies, specifically as an anode material in lithium-ion batteries (LIBs). With the growing global demand for electric vehicles (EVs) and supply risks, finding alternative sources has become necessary. Waste carbon (WC) materials, which have significant graphite content, offer a promising secondary source for battery applications. Despite developments in recycling technologies, most efforts remain focused on cathode materials from spent LIBs and rely on corrosive leaching agents that are challenging to manage and impact the environment through emissions. Thus, it is essential to advance research focused on waste carbon recycling, and this study seeks to develop a green leaching technology using ascorbic acid to purify waste carbon, particularly graphitic waste from the Acheson furnace, with about 99.85% purity. The effectiveness of ascorbic acid has been investigated for removing impurities like Fe, Al, Ca, and S. A 2-level factorial design was employed using Stat-Ease Design Expert (DOE) software to identify the significant factors and interactions between selected variables such as acid concentration, temperature, and time. The effective removal of Fe, Al, Ca, and S using ascorbic acid leaching demonstrated the potential to enhance the graphite purity to >99.95%, meeting the minimum purity required for battery-grade applications.

## 1 Introduction

Graphite materials are utilized in a wide range of applications, from conventional uses such as writing tools and refractories to modern technologies including portable electronics and electric vehicles (EVs) [1-3]. This versatility stems from the unique structure of graphite, composed of sp<sup>2</sup>-hybridised carbon (C) atoms arranged in a hexagonal layered lattice [2]. This arrangement leads to different types of atomic interactions within graphite, with each contributing specific functional roles and properties. The  $\sigma$ -bonds, formed by the direct overlap of sp<sup>2</sup> orbitals, hold the C atoms together within each 2D layer, enabling high thermal conductivity along the layers [2,4,5]. Meanwhile, the  $\pi$ -bonds, resulting from the sideways overlap of p-orbitals, create a shared  $\pi$ -electron cloud within each layer, which facilitates high electrical conductivity along the plane [2,4,5]. The layers are held together by weak van der Waals forces, forming the anisotropic layered structure of graphite [2,4,5].

The distinct combination of atomic interactions within graphite allows it to effectively intercalate ions, maintaining structural integrity during the reversible process [6]. This property makes graphite highly suitable for battery applications. As a result, graphite has become the primary anode material for lithium-ion batteries (LIBs) [1,7-9], typically about 12-22% w/w of active material [5,9-12].

From 2006 to 2011, graphite used as anode materials for LIBs had a lower market value compared to conventional carbon products [13]. However, over the past decade, the market has shifted towards the LIB industry as the demand for portable devices and EVs increases, driven by the need for efficient rechargeable energy storage [7,9,14]. As a result, the United States (US), European Union (EU), and Australia recognized graphite as a critical material [3,5,7,15,16], highlighting its growing global importance.

Commercial graphite anodes are mainly sourced from natural graphite (NG), which is mined from ores, and synthetic graphite (SG), produced by high-temperature graphitization of carbon-rich materials, resulting in about 97 – 99.9% purity [1,2,5,9,14,17], almost meeting the 99.95% minimum purity requirement of LIB anodes [1,5]. However, with graphite now classified as a critical material, the need for securing a sustainable supply has become even more pressing. This urgency is driven by China's dominant position in global graphite production (~79%) and reserves (~28%) [3,5]. Given the growing global demand and supply dependence, concerns over potential instability in supply, trade, and prices have grown [5]. Thus, finding alternative sources has become necessary to support the demands of existing and emerging technologies.

The alternative graphite sources are categorized as secondary sources of graphite, and this study used the

\* Corresponding author: [richard.alorro@curtin.edu.au](mailto:richard.alorro@curtin.edu.au)

waste carbon (WC) provided by the industry partner to investigate the potential of using ascorbic acid in the purification of graphite to meet the 99.95% purity for anode applications

## 2 Experimental

### 2.1 Materials and characterization

The waste carbon (WC) sample, provided by an industry partner, is a material from the Acheson graphitization furnace, and identified in this experiment as WC-D. The ascorbic acid used in the leaching experiment is of analytical grade. The particle size distribution was analyzed using a laser diffraction particle size analyzer. The mineralogy and elemental composition were obtained by a commercial lab using Quantitative X-ray Diffraction (QXRD) and assay via Inductively Coupled Plasma - Optical Emission Spectrometry/Mass Spectrometry (ICP-OES/MS). The raw sample morphology and general presence of impurity were obtained via Scanning Electron Microscopy (SEM) using Secondary Electrons (SE) and Backscattered Electrons (BSE). The experiments were designed using Stat-Ease Design Expert (DOE) software. The leaching solutions were analyzed using ICP-OES and utilized in the DOE.

### 2.2 Leaching experiments

The experiments involved a single-acid leaching for WC-D using ascorbic acid with 2-level factors of acid concentrations, reaction times, and temperature. The solid-to-liquid ratio and stirring rate were fixed at 2% (g of sample / mL of solution) and 200 rpm, respectively. The leaching experiments were conducted using a 50-ml Erlenmeyer flask placed in a water bath on a single hotplate stirrer. Solid-liquid separation was done via filtration, where the liquid solutions analyzed by ICP-OES. The removal efficiency (or leaching efficiency) was computed using Equation 1.

$$\%R = \frac{C_{metal} \cdot V_{solution}}{C_0 \cdot m_{sample}} \times 100 \quad (1)$$

In Equation 1, %R is the elemental removal (%),  $C_{metal}$  is the metal concentration in leaching solution (mg/L),  $V_{solution}$  is the volume of leaching solution (L),  $C_0$  is the initial metal content of the feed (ppm, mg/kg), and  $m$  is the mass of the WC feed (g).

The leaching runs were done in random order with 2 replicates, following the design made through DOE, with the 2-level factors summarized in Table 1.

**Table 1.** Single-acid leaching with 2-level factors for WC-D using ascorbic acid.

| Factor              | Low (L) | High (H) |
|---------------------|---------|----------|
| A: Time, h          | 1       | 6        |
| B: Concentration, M | 0.5     | 1.5      |
| C: Temperature, °C  | 25      | 60       |

Only the dissolutions of Fe, Al, Ca, and S were selected due to the relatively higher concentrations in the WC sample, meeting the detection limit of the ICP-OES. The results shows the effectivity of ascorbic acid in removing the impurities, especially for Fe, which has the highest concentration among the impurities.

## 3 Results and discussion

### 3.1 Sample characterization

The mineralogy and elemental composition of the WC sample was analyzed through a commercial lab using QXRD and assay via ICP-OES/MS. The QXRD analysis identified graphite as the major mineral in the WC sample, accounting for 100% as shown in Fig. 1.

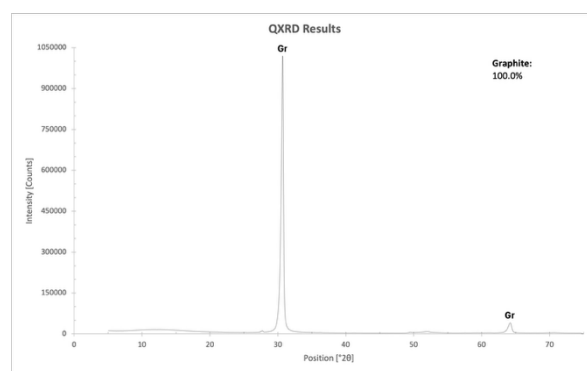


**Fig. 1.** QXRD results for WC-D (Co K $\alpha$ , 1.789Å)

The bulk assay via ICP-OES/MS provided more information on the elemental composition and quantity of the impurities in the WC sample. The result in Fig. 2 shows that the major impurities are Fe, S, Al, and Ca, accounting for ~0.136%, and removing these may increase the purity from ~99.85% to ~99.99%. Since the impurity concentrations are very low, focus is given to the major impurities, especially with Fe. The challenges encountered and recommendations are discussed in Section 4.

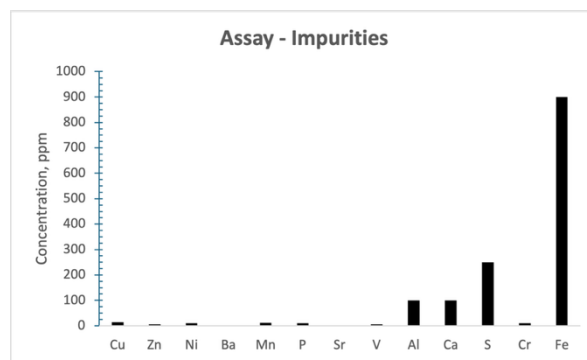


**Fig. 2.** Selected WC-D impurities in ppm range.

The PSD was analyzed using a laser diffraction particle size analyzer, and as shown in Fig. 3, the particle size at 90% passing ( $P_{90}$ ) for WC-D is approximately 65 $\mu$ m. With this size range, no further size reduction was conducted prior to leaching.

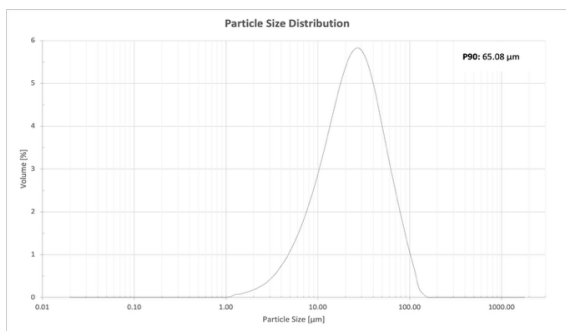


**Fig. 3.** Particle size analysis for WC-D.

The SEM SE image presented in Fig. 4a confirms the size analysis results and reveals that WC-D has a plate-like structure, which is advantageous for the leaching process. The open structure allows access to the impurities, promoting their removal. The SEM BSE image in Fig. 4b illustrates the presence of impurities, which are distinguishable through elemental contrast. Graphite or carbon (C) appears darker due to its lower atomic number, while the impurities appear brighter due to their higher atomic number. The limited presence of brighter particles aligns with the low concentrations observed in the assay analysis.

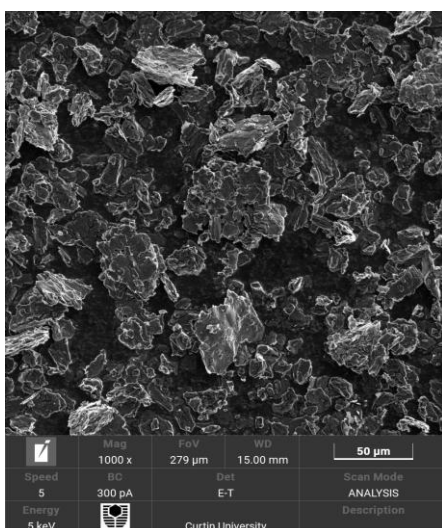


**Fig. 4a.** SEM SE imaging at 500x magnification.

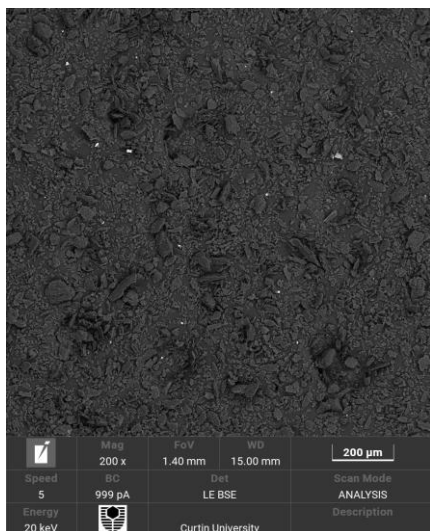


**Fig. 4b.** SEM BSE imaging at 200x magnification.

### 3.2 Significant factors and interactions

The significant factors in leaching each impurity using ascorbic acid were identified via DOE. Table 2 summarizes the different significant factors, including their interactions, while Fig. 5a to 5d present the one-factor and 3D plots obtained from DOE.

In leaching Fe, temperature was identified as a significant factor. The plot in Fig. 5a shows a clear positive trend, with Fe removal increasing with temperature, reaching the highest efficiency at 60 °C.

For Al, both time and temperature were significant, with interaction showing that removal is better at higher temperatures, even at 1-hour leaching time. The 3D plot in Fig. 5b shows that temperature has a steeper gradient, indicating it has more influence on Al dissolution than time. This means that elevating the temperature is more effective in enhancing efficiency than extending the leaching time alone.

In the case of Ca, all three factors (time, concentration, temperature) were found to be significant, with interaction effects between time and temperature. Similar to Al, the removal of Ca is also better at higher temperatures, even at a 1-hour leaching time, as shown in Fig. 5c.

For S removal, concentration was significant. The plot in Fig. 5d presents a positive effect in leaching S with concentration, reaching the highest efficiency at 1.5 M.

**Table 2.** Significant factors identified via DOE for single-acid leaching using ascorbic acid.

| Impurity | Significant Factors                  | Interaction        |
|----------|--------------------------------------|--------------------|
| Fe       | Temperature                          | –                  |
| Al       | Temperature<br>Time                  | Time–Temperature   |
| Ca       | Temperature<br>Time<br>Concentration | Time–Concentration |
| S        | Concentration                        | –                  |

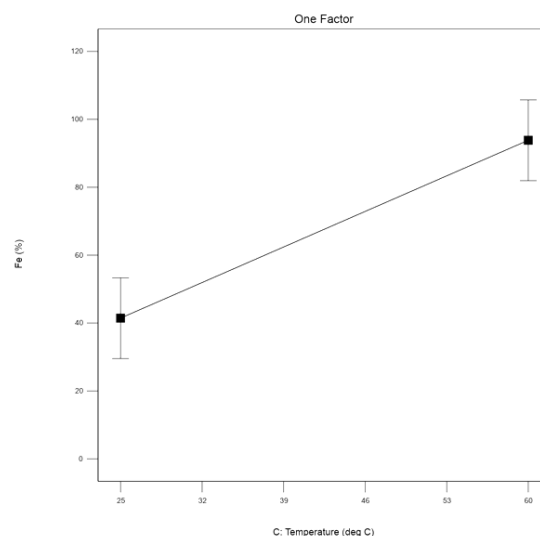


**Fig. 5a.** DOE Fe results for WC-D using ascorbic acid: temperature plot.

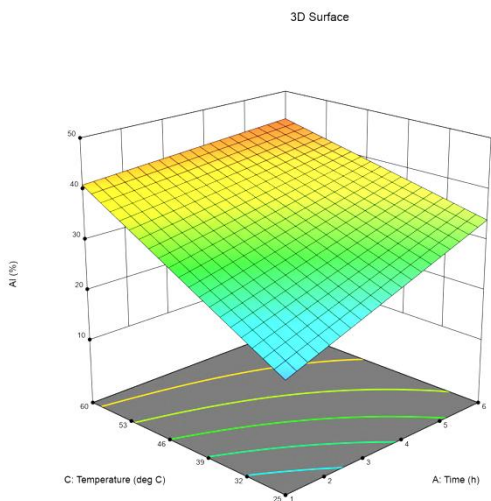


**Fig. 5b.** DOE Al results for WC-D using ascorbic acid: 3D plot of time-temperature interaction.

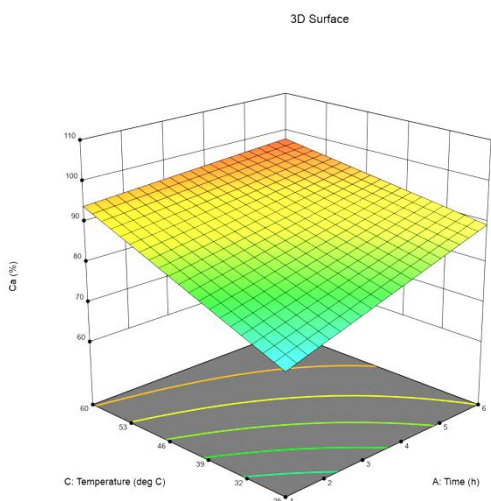


**Fig. 5c.** DOE Ca results for WC-D using ascorbic acid: 3D plot of time-temperature interaction.

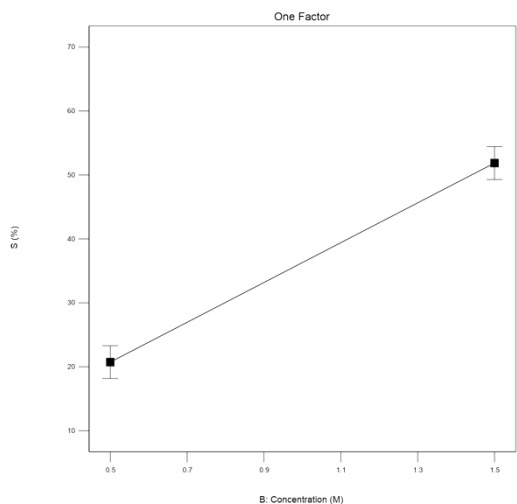


**Fig. 5d.** DOE S results for WC-D using ascorbic acid: concentration plot.

### 3.3 Leaching efficiency and graphite purity

The highest removal of Fe, Al, Ca, and S was achieved at 6 h, 1.5 M, and 60 °C, with an estimated efficiency of ~100%, ~43%, ~100%, and ~59%, respectively. With this, the purity of WC-D has been potentially improved to >99.95%, meeting the minimum purity requirement of graphite anodes.

This result is supported by the SEM BSE images in Figures 4b and 6, where the reduction of brighter particles is evident after leaching, verifying the removal of impurities.

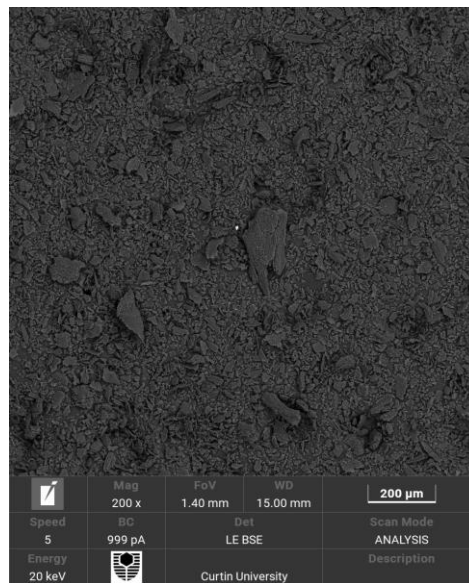


**Fig. 6.** SEM BSE imaging of WC-D product at 200x magnification

## 4 Conclusion

Ascorbic acid has the potential to purify graphite in single-acid systems, particularly for Fe, Al, Ca, and S, with an estimated efficiency of ~100%, ~43%, ~100%, and ~59%, respectively. This result has potentially increased the WC purity to >99.95%, meeting the minimum requirement for graphite anodes. Among the impurities, the removal of Fe had the highest impact with its initial concentration in the WC-D sample, and the plate-like open structure allowed access to these impurities, promoting their removal.

The use of Stat-Ease software (DOE) has been helpful in designing the experiments, especially for screening multiple variables in systems with trace-level impurities, ensuring statistically reasonable results that help understand the system despite experimental limitations.

Overall, this initial test work may be continued for scale-up experiments, investigate other factors with multiple levels, optimize identified significant factors, and explore other organic acids

This research was funded by the Research Institute of Industrial Science and Technology (RIST), Republic of Korea, under the project grant number RES-SE-WAS-DP-66242-1.

Part of this research was undertaken using the FESEM instrumentation (ARC LE190100176) at the John de Laeter Centre, Curtin University.

## References

1. Frohs, W.; Jäger, H. Industrial carbon and graphite materials : raw materials, production and applications; Wiley-VCH: Weinheim, Germany, 2021.
2. Pierson, H.O. Handbook of Carbon, Graphite, Diamond, and Fullerenes: Properties, Processing, and Applications; Noyes Publications: 1993.
3. U.S. Geological Survey. Mineral commodity summaries 2025; 2025; Reston, VA, 2025; p. 212.
4. Chung, D.D.L.; Wca. Review Graphite. Journal of materials science 2002, **37**, 1475 – 1489, doi: <https://doi.org/10.1023/A:1014915307738>.
5. Bondoc, M.J.; Jorolan, J.H.; Eom, H.-S.; Lee, G.-G.; Alorro, R.D. Advances in Graphite Recycling from Spent Lithium-Ion Batteries: Towards Sustainable Resource Utilization. Minerals 2025, **15**, doi: <https://doi.org/10.3390/min15080832>.
6. Li, Y.; Lu, Y.; Adelhelm, P.; Titirici, M.-M.; Hu, Y.-S. Intercalation chemistry of graphite: alkali metal ions and beyond. Chemical Society Reviews 2019, **48**, 4655 – 4687, doi: <https://doi.org/10.1039/C9CS00162J>.
7. Bauer, D.; Khazdozian, H.; Mehta, J.; Nguyen, R.T.; Severson, M.H.; Vaagensmith, B.C.; Toba, L.; Zhang, B.; Hossain, T.; Sibal, A.P.; et al. 2023 Critical Materials Strategy; United States, 2023.
8. ECGA. ECGA Annual Report 2022; European Carbon and Graphite Association: Brussels, Belgium, April 16, 2023 2023.
9. Natarajan, S.; Divya, M.L.; Aravindan, V. Should we recycle the graphite from spent lithium-ion batteries? The untold story of graphite with the importance of recycling. Journal of energy chemistry 2022, **71**, 351-369, doi: <https://doi.org/10.1016/j.jechem.2022.04.012>.
10. Gao, Y.; Zhang, S.; Lin, S.; Li, Z.; Chen, Y.; Wang, C. Opportunity and challenges in recovering and functionalizing anode graphite from spent lithium-ion batteries: A review. Environmental Research 2024, 118216, doi:<https://doi.org/10.1016/j.envres.2024.118216>.
11. Golmohammadzadeh, R.; Faraji, F.; Rashchi, F. Recovery of lithium and cobalt from spent lithium ion batteries (LIBs) using organic acids as leaching reagents: A review. Resources, conservation and recycling 2018, **136**, 418-435, doi: <https://doi.org/10.1016/j.resconrec.2018.04.024>.
12. Velázquez-Martínez, O.; Valio, J.; Santasalo-Aarnio, A.; Reuter, M.; Serna-Guerrero, R. A Critical Review of Lithium-Ion Battery Recycling Processes from a Circular Economy Perspective. Batteries 2019, **5**, 68.
13. Fetherston, J.M. Graphite in Western Australia. 2015, **84**.
14. Hughes, A.; Britt, A.; Pheaney, J.; Morfiadakis, A.; Kucka, C.; Colclough, H.; Munns, C.; Senior, A.; Cross, A.; Hitchman, A.; et al. Australia's Identified Mineral Resources 2024; 2025.
15. European Commission; Directorate-General for Internal Market, Industry Entrepreneurship; Smes; Grohol, M.; Veeh, C. Study on the critical raw materials for the EU 2023 – Final report; Publications Office of the European Union: 2023.
16. Jara, A.D.; Betemariam, A.; Woldetinsae, G.; Kim, J.Y. Purification, application and current market trend of natural graphite: A review. International Journal of Mining Science and Technology 2019, **29**, 671-689, doi:<https://doi.org/10.1016/j.ijmst.2019.04.003>.
17. Scherba, C.; Montreuil, J.-F.; Barrie, C.T. Chapter 15 Geology and Economics of the Giant Molo Graphite Deposit, Southern Madagascar. 2018; pp. 347-363.